Effects of Adult-Generated Granule Cells on Coordinated Network Activity in the Dentate Gyrus

Clay O. Lacefield,[1] Vladimir Itskov,[1,2] Thomas Reardon,[2]
René Hen,[1,3,4]* and Joshua A. Gordon[3,4]*

ABSTRACT: Throughout the adult life of most mammals, new neurons are continuously generated in the dentate gyrus of the hippocampal formation. Recent work has documented specific cognitive deficits after elimination of adult hippocampal neurogenesis in rodents, suggesting that these neurons may contribute to information processing in hippocampal circuits. Young adult-born neurons exhibit enhanced excitability and have altered capacity for synaptic plasticity in hippocampal slice preparations in vitro. Still, little is known about the effect of adult-born granule cells on hippocampal activity in vivo. To assess the impact of these new neurons on neural circuits in the dentate, we recorded perforant-path evoked responses and spontaneous network activity from the dentate gyrus of urethane-anesthetized mice whose hippocampus had been focally X-irradiated to eliminate the population of young adult-born granule cells. After X-irradiation, perforant-path responses were reduced in magnitude. In contrast, there was a marked increase in the amplitude of spontaneous γ-frequency bursts in the dentate gyrus and hilus, as well as increased synchronization of dentate neuron firing to these bursts. A similar increase in gamma burst amplitude was also found in animals in which adult neurogenesis was eliminated using the GFAP:TK pharmacogenetic ablation technique. These data suggest that young neurons may inhibit or destabilize recurrent network activity in the dentate and hilus. This unexpected result yields a new perspective on how a modest number of young adult-generated granule cells may modulate activity in the larger population of mature granule cells, rather than acting solely as independent encoding units. © 2010 Wiley Periodicals, Inc.

KEY WORDS: dentate gyrus; adult neurogenesis; gamma oscillations; in vivo multielectrode recording; input–output curves

INTRODUCTION

Adult neurogenesis in the dentate gyrus of the hippocampus is a process by which new granule cells are continuously generated and integrate within circuits of mature cells in the region. First documented by Altman and Das (1965) in their early characterization of patterns of development in the brain, adult hippocampal neurogenesis has of late become of particular interest to neuroscientists for its possible relevance to high-level neural processes such as mood regulation and learning (Malberg et al., 2000; Santarelli et al., 2003; Becker and Wojtowicz, 2007; Sahay and Hen, 2007).

Studies in experimental animals have assessed the behavioral consequences of disrupting adult hippocampal neurogenesis using a variety of ablation techniques. These have shown that neurogenesis may support hippocampal-dependent behaviors such as contextual fear conditioning (Saxe et al., 2006; Deng et al., 2009), specific Morris water maze paradigms (Snyder et al., 2005; Zhang et al., 2008; Deng et al., 2009), and spatial pattern separation (Clelland et al., 2009). Behavioral effects in these tasks have also been demonstrated from specific genetic perturbations of other components of the dentate gyrus/CA3 network (McHugh et al., 2007; Nakashiba et al., 2008), suggesting that young neurons have a role consistent with the overall function of this intrinsic hippocampal circuit.

Like young neurons generated during development, young adult-generated granule cells possess properties distinct from those of mature neurons. From the time that they receive their first perforant-path synapses until they are almost fully mature (from 2- to 4-weeks postdivision), young granule cells have lower thresholds for firing action potentials and long-term potentiation (LTP) than mature neurons (Wang et al., 2000; Schmidt-Hieber et al., 2004; Esposito et al., 2005; Laplagne et al., 2006; Ge et al., 2007). Furthermore, young neurons appear to mediate "ACSF-LTP," a form of dentate field LTP that is induced in hippocampal slices bathed in artificial cerebrospinal fluid (ACSF) in the absence of the inhibitory antagonists typically used in the study of dentate LTP in vitro (Snyder et al., 2001; Saxe et al., 2006). This suggests that young neurons may selectively undergo LTP when mature neurons do not, such as when they are subject to the strong inhibition characteristic of the DG both in vitro and in vivo (Dudek et al., 1976; Wigstrom and Gustafsson, 1983; Snyder et al., 2001; Ge et al., 2008). Consequently, the notion has arisen that the enhanced plasticity and excitability of young

neurons makes them a preferential substrate for new memories or representations (Doetsch and Hen, 2005; Aimone et al., 2006, 2009; Kee et al., 2007; Tashiro et al., 2007).

Thus far however, most of what we know about the impact of adult neurogenesis on hippocampal circuits comes from electrophysiological recordings in acute slices from rodent hippocampus. But what do we really know about the effects that young neurons have on neural circuits in vivo? To enhance our understanding of the role of young adult-born neurons in the intact hippocampus, we conducted a series of neural recordings in urethane-anesthetized mice after focal hippocampal X-irradiation, a robust technique for selective elimination of the population of young neurons that resides in the dentate gyrus (Santarelli et al., 2003). We report here evidence of reduced efficacy of perforant path inputs to the dentate gyrus following X-irradiation, in the form of decreased input–output relationships in the irradiated animals. In these same animals, we find an increase in the amplitude of synchronous gamma bursts, the predominant form of coordinated network activity in the dentate gyrus under urethane anesthesia. The increased gamma burst amplitude is accompanied by increased single unit synchrony within the dentate gyrus. To rule out nonspecific effects of irradiation, we confirm the increases in gamma burst amplitude in animals where adult neurogenesis is eliminated by an independent method, pharmacogenetic ablation using GFAP:TK transgenic mice (Saxe et al., 2006). Finally, we establish that these bursts are indeed dependent upon perforant-path activity by silencing inputs from the entorhinal cortex. These findings raise the intriguing possibility that integration of new units into the adult dentate gyrus has a distinct effect on networks in the dentate at the circuit level that cannot be predicted from what is currently known about the properties of young neurons individually. Knowledge of how adult neurogenesis affects neural activity on the network level may help understand the role of adult-born dentate neurons in hippocampal function.

MATERIALS AND METHODS

X-Ray Irradiation

To examine the role of adult-generated dentate granule cells in hippocampal network activity, we performed local field potential (LFP) recordings in 25 X-ray-irradiated and 22 sham-irradiated C57/Bl6 mice (Jackson Labs, Bar Harbour, Maine). While many previous studies of adult hippocampal neurogenesis in mice have used the 129sv/ev mouse strain (Santarelli et al., 2003; Saxe et al., 2006), we chose to use C57 animals due to their higher baseline levels of neurogenesis (Kempermann et al., 1997), to maximize our chances of seeing differences between the groups after irradiation. Recent work from our lab has furthermore confirmed that key behavioral defects after X-irradiation are similar in C57 and 129 strains of mice (David et al., 2009). The irradiation procedure was performed as detailed previously (Santarelli et al., 2003; Saxe et al., 2006),

and involved three doses of five Grays of X-rays, given at 2-day intervals. Irradiation was performed under Ketamine/Xylazine anesthesia (15 and 5 mg/kg, respectively) through a lead shield custom-fabricated with a window above the hippocampus, fitted into a standard stereotaxic frame. Male animals were X-irradiated at 6 weeks of age and experiments were performed from 6 to 10 weeks after irradiation to allow for any acute effects of irradiation to subside. In these conditions, irradiation produces a complete abolition of neurogenesis, as measured by Bromodeoxyuridine (BrdU) and Doublecortin (DCX) immunohistochemistry (Supporting Information Fig. 1A, performed as described in Saxe et al., 2006). In addition, no evidence of X-ray-induced inflammation can be detected at this time point (Meshi et al., 2006). Control sham-irradiated animals were littermates subjected to similar handling and anesthesia but without irradiation. All procedures were performed according to NIH guidelines for care and handling of experimental animals and approved by the Institutional Animal Care and Use Committees of Columbia University and the New York State Psychiatric Institute.

GFAP:TK Ablation

Mice carrying transgenes with the thymidine kinase gene under control of the glial fibrillary acid protein promoter (GFAP:TK; described in Saxe et al., 2006) were backcrossed six generations onto the C57/BL6 strain background. Male mice from 6 to 8 weeks of age were implanted with a series of three 28-day subcutaneous mini-osmotic pumps (Alzet) containing 25 mg ml^{-1} ganciclovir in 0.9% saline (effective dose 66 μg day^{-1}). Recording of spontaneous network activity with linear silicon probes in urethane anesthetized animals was performed blind to genotype in eight 4- to 5-month old mice carrying the GFAP:TK transgene as well as eight similarly implanted wild-type littermates. All mice received ganciclovir. Elimination of adult neurogenesis was confirmed by immunohistochemical staining for markers of young neurons (e.g., DCX) in brain slices from animals subjected to recording (Supporting Information Fig. 1B).

Surgery and In Vivo Electrophysiology

For acute electrode implantation and recording, animals were weighed and anesthetized with 1.8 mg kg^{-1} urethane and placed in a small-animal stereotaxic frame. A small craniotomy was made over the dorsal hippocampus and a single-wire tungsten electrode (0.5 MΩ, 125-μm diameter, AM systems, Sequim, WA; used in 21 animals) or 16-channel linear probe array (50-μm spacing; 15-μm thick, 150-μm wide shank, NeuroNexus Technologies, Ann Arbor, MI; used in 26 animals) was lowered into the dentate gyrus (in mm, AP: −1.4, ML: −1.1, DV: −2.3; see Supporting Information Fig. 2A). Another small craniotomy was performed over the ipsilateral angular bundle and a bipolar concentric stimulating electrode (MCE-100; 150-μm diameter, Rhodes Medical Instruments, Summerland, CA) poised for implantation into the perforant path (AP: lambda, ML: −2.6, DV: −1.6 mm; see Supporting Information Fig. 2B) after completing the acquisition of spontaneous local field potential activity.

The silicon probe arrays provided a more complete picture of spatial patterns of network activity throughout the dentate gyrus and hilus than single-wire electrodes, enabling us to perform current-source density analyses (CSDs) of laminar activity profiles (Nicholson and Freeman, 1975). These probes also allowed us to observe the spiking activity of multiple single units after clustering spike waveforms between successive electrodes in the 50-μm-spacing array. Data were collected at least 15 min after probe implantation.

To quantify network activity, signals from 10 min of recording immediately prior to stimulating electrode insertion were acquired in nine irradiated and nine sham animals using the linear probe array. Local field potentials were amplified using customized EEG amplifiers (Grass Instruments, West Warwick, RI), (filtered for 0.1 Hz to 20 kHz), sampled at 32 kHz with a National Instruments AD board, and acquired with custom software written using Lab-View (National Instruments, Austin, TX). Data were imported into MATLAB (Mathworks, Natick, MA) and downsampled to 1 kHz for analysis of local field potentials using custom software adapted from programs written by Ken Harris (Rutgers) and Partha Mitra (Cold Spring Harbor). For single unit determination, spike waveforms were clustered with the Klusters software package (freely available from the Buzsaki laboratory, http://osiris.rutgers.edu) after filtering of the broadband signals for spikes (350–5,000 Hz) and spike extraction with custom MATLAB scripts. All subsequent analyses and statistics of local field potentials (LFPs) and spike firing were performed using MATLAB.

In all experiments, gamma activity was quantified from the probe site located in the hilar region, identified as the channel showing the largest positive field potential response to perforant path stimulation (e.g., Supporting Information Fig. 2A, Channel 14). Gamma power was calculated as the sum of the power spectral density in the 25- to 80-Hz frequency range in the hilar electrode LFP over the entire 10-min recording, using the Welch method for power estimation (2 s windows). For quantification of gamma burst amplitudes and frequency several methods were used to identify bursts and all yielded similar results. Gamma bursts were identified by finding peaks in instantaneous gamma power (calculated using a multi-taper time–frequency power spectrogram with a time window size of 100 ms) that exceeded a threshold of 1 standard deviation above the mean power for the frequency range of 25–80 Hz (Supporting Information Fig. 4). The increase in gamma burst magnitude after X-irradiation was consistent across a broad range of detection thresholds, whether using a multiple of the standard deviation or an absolute measure (Supporting Information Fig. 5). Frequency comparisons differed based upon the detection method and were inconclusive.

Current-source density (CSD) analyses were performed by calculating the second derivative of a third-degree polynomial fit of the LFP data. Group CSDs of gamma burst activity were calculated on average gamma burst LFPs for each animal, identified in the same manner as in Supporting Information Figure 4, described above.

Analysis of spiking activity of identified single-units was limited to units located near the hilar electrode used for gamma burst quantification (Supporting Information Fig. 6), however we were unable to unambiguously classify these as either granule cells or interneurons. The activity of multiple single-units in the granule cell layer/hilar region was analyzed with respect to gamma bursts in the hilar local field potential, which were identified as described above. Phase relationships of unit firing to the underlying theta envelope of the gamma bursts were quantified using the Rayleigh's z-statistic. Gamma epochs were assessed as periods with gamma power over 0.5 standard deviations above the mean.

Perforant-Path Evoked Responses

Perforant path stimulation was performed using a constant-current stimulus isolation unit (World Precision Instruments, Sarasota, FL) triggered by the pClamp Clampex software through an Axon Digidata 1322a interface (Molecular Devices, Sunnyvale, CA). Evoked responses were recorded either from the hilus using the single-wire electrode, whose position was optimized to measure the maximum positive field response, or from all 16 probe channels throughout the layers of the dentate/hilar region. In both cases, responses were acquired using the Axon Clampex package and analyzed with the associated Clampfit analysis software. Baseline stimuli ranging from 200 to 400 μA with a 100-ms pulse duration were delivered at 0.03 Hz to optimize the stimulating electrode position. For input–output curves, the slope of the evoked field potential was calculated from the linear portion of the rising phase of the electrode contact located in the hilus, as has been described in previous work, over a stimulus range of 0–400 μA (20-μA increments, 0.03 Hz), (Namgung et al., 1995; Jones et al., 2001).

Recordings of paired-pulse facilitation (PPF) and paired-pulse inhibition (PPI) were performed in a similar manner to input–output curves except that stimuli were given at 0.016 Hz and stimulus strength was maintained at either of two levels while the interstimulus interval (ISI) of the pair of pulses was varied between 10 and 100 ms (in 5-ms increments). For paired-pulse facilitation, stimulus intensity was adjusted to produce a 1- to 2-mV field potential response on the initial pulse of the pair. The relative amplitude of the second evoked field potential was measured for PPF calculation. For paired-pulse inhibition, one measure of feedback inhibition in the dentate, the stimulus intensity was set such that a 1- to 2-mV population spike (popspike) was generated by the first pulse. In this case the relative amplitude of the second popspike in response to the subsequent pulse of stimulation was measured.

Perforant-Path Inactivation

Experiments inactivating perforant-path inputs to the dentate gyrus using tetrodotoxin (TTX) were performed on six irradiated and five sham animals in identical conditions to the aforementioned recordings, except that stimulation was performed with a custom-made bipolar 75-μm tungsten electrode bonded 0.2-mm past the end of a 33-gauge cannula. After electrode implantation, LFPs were recorded for 10 min at 32 kHz to observe network activity prior to TTX administration. The stimulating electrode-cannula assembly was then used to stimulate the angular bundle to perform an initial input–output curve, following which TTX was slowly infused over the course

of 5 min (0.5 μl, at 5 ng/μL; Sigma #T5651, St. Louis, MO). The perforant-path was stimulated at 0.03 Hz at maximal response intensity and the evoked responses recorded to observe the TTX-induced decrement of the evoked potential in the hilus; only experiments in which the TTX completely abolished the perforant path evoked responses were used. At this time, another 10-min recording was performed to quantify dentate gyrus network activity following inactivation of ipsilateral perforant-path input to the hippocampus.

RESULTS

To examine the effects of adult neurogenesis on hippocampal networks in vivo, we performed a series of electrophysiological recordings in urethane-anesthetized adult mice whose hippocampus had been focally X-irradiated to eliminate the generation of new neurons. We recorded both evoked responses and spontaneous network activity using either single-wire tungsten electrodes or linear silicon electrode arrays in order to sample local field potentials in the dentate gyrus and hilus.

Dentate Gyrus Responses to Perforant-Path Input in X-Irradiated Mice

Since young adult-born granule cells have been shown to exhibit enhanced excitability (Schmidt-Hieber et al., 2004; Mongiat et al., 2009), we first hypothesized that eliminating the population of young neurons with X-irradiation would decrease field evoked responses to perforant path stimulation. Dentate population field responses to stimulation of the perforant path were recorded and quantified in vivo in urethane-anesthetized mice subjected to focal X-irradiation or a sham procedure. Input–output relationships in the hilus of irradiated animals were reduced modestly but significantly (Fig. 1a, $P < 0.05$ for effect of X-irradiation, repeated measures analysis of variance (ANOVA) over entire stimulation intensity range; stimulation intensity at [1/2] max was 60 μA vs. 100 μA for X-ray and sham, respectively). Despite this reduction in evoked population responses after irradiation, no differences were readily apparent in subsequent measures of short term synaptic facilitation or paired-pulse inhibition of population spiking activity (Figs. 1b,c).
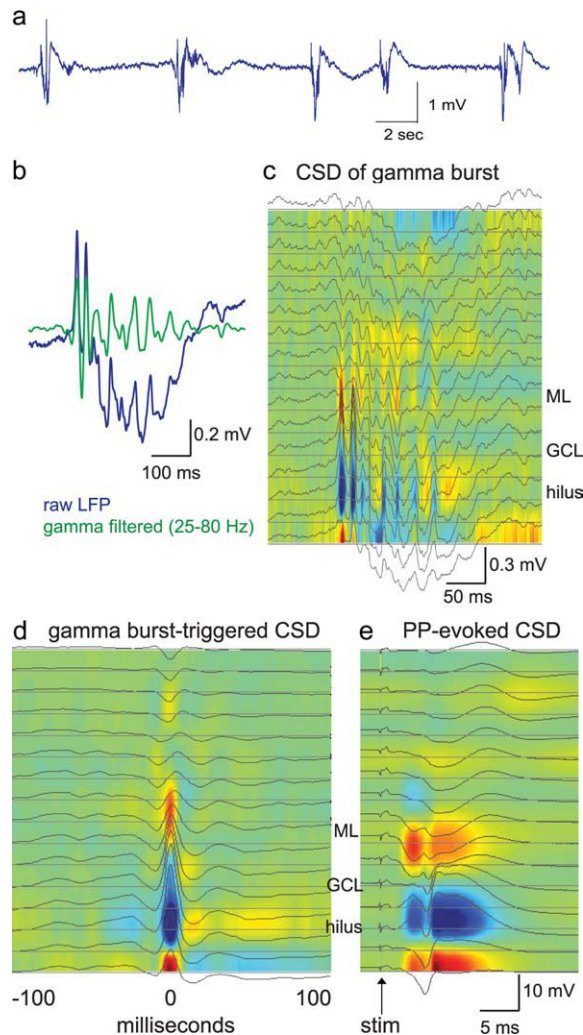
Spontaneous Network Activity in Irradiated Mice: Dentate Gamma Bursts

We next examined the effects of X-irradiation on spontaneous network activity in the dentate gyrus. In C57/Bl6 mice, spontaneous activity in the dentate gyrus and hilar regions under urethane anesthesia is marked by bursts of activity evident in the local field potential (LFP), similar in some respects to CA1 sharp waves (Fig. 2a). As has been documented previously in rats (Bragin et al., 1995; Isomura et al., 2006), these complex LFP bursts consist of a strong gamma frequency (25–80 Hz) component riding on top of a lower frequency enve-
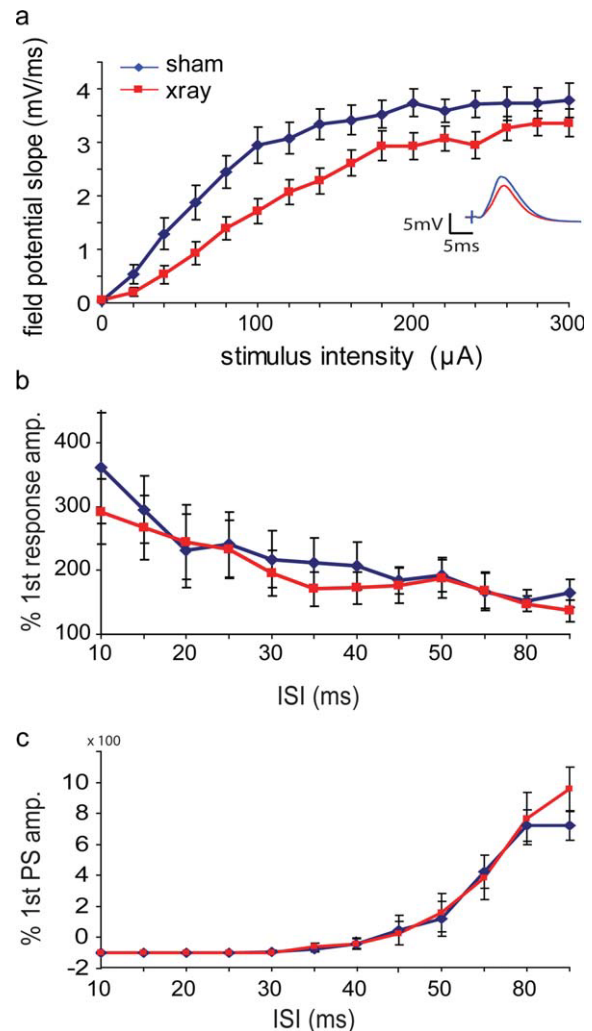
FIGURE 1. Effects of focal hippocampal X-irradiation on perforant-path evoked responses. (a) Input–output curves of evoked field potential slope in response to stimulation of the angular bundle. X-irradiated animals (red lines) exhibit decreased responses to perforant path input compared with sham animals (blue lines), ($n = 19$ X-ray, 17 sham animals; $P < 0.05$, repeated measures ANOVA over entire range). Inset: average hilar field potential responses at 100-μA stimulation intensity. (b) Paired pulse facilitation was similar between the two groups, indicating no change in presynaptic function after irradiation. (c) Feedback inhibition was also unchanged, as assayed though paired-pulse inhibition of the second population spike when presented with two suprathreshold stimuli in rapid succession. [Color figure can be viewed in the online issue, which is available at wileyonlinelibrary.com.]

lope of around theta range (3–8 Hz). Because of the characteristic gamma activity associated with these dentate slow oscillations they are often referred to as "gamma bursts," though spectral analysis shows that they are comprised of diverse frequency components (Supporting Information Fig. 3). Current-source density (CSD) analysis of these bursts using linear electrode arrays revealed that they were indeed accompanied by large γ-frequency current sinks and sources localized to the dentate/hilar region (Figs. 2c–e), supporting prior findings that

FIGURE 2.   Characterization of spontaneous network activity in the DG of urethane anesthetized mice. (a) Raw LFP trace from a hilar recording electrode showing a series of spontaneous gamma bursts. Bursts occurred at an average of ~1 Hz in both groups (see Supporting Information Fig. 5). (b) Raw (blue) and γ-filtered (green) LFP trace from a single gamma burst. The γ-filtered trace was band-pass filtered at 25–80 Hz. (c) Current-source density analysis of the same gamma burst as in "B," over all 16 electrodes in the probe array, at 50-μm spacing. Current sinks, denoting influx of positive charge, are marked in red, while current sources are labeled in blue. (d) CSD of average gamma peak-triggered LFP from all gamma bursts from the experiment shown in Panels a–e. (e) CSD of perforant-path evoked stimulation from the same experiment as Panels b–d. Note that the pattern of sources and sinks during gamma bursts is generally similar to that evoked by perforant-path stimulation. Error bars are S.E.M. throughout. [Color figure can be viewed in the online issue, which is available at wileyonlinelibrary.com.]

this type of activity originates locally in the dentate and is not merely propagated to the region by volume conduction.

Gamma bursts were present in both sham and X-irradiated mice, and the source/sink structure of these bursts were qualitatively similar (Figs. 3a,b). To test for quantitative differences in network activity between the two groups, we first measured

overall gamma power. Gamma power was elevated in the irradiated animals as compared with sham animals (0.0028 ± 0.0008, 0.00077 ± 0.00033 mV^2 Hz^{-1}, for nine X-ray and nine sham animals, respectively; mean ± S.E.M., $P = 0.04$, two-tailed Student's t-test). Such an increase in gamma power could arise from an increase in burst frequency and/or amplitude. To measure these properties, we identified individual bursts by detecting the peaks in gamma power in the hilar electrode that accompany these epochs (Supporting Information Fig. 4). Burst amplitude was then calculated by measuring the peak-to-trough voltage amplitude of each individual burst within the epoch. In animals lacking adult hippocampal neurogenesis, gamma bursts occurred at a comparable frequency but were significantly larger on average (Fig. 3a, burst amplitudes, $P = 0.001$, two-tailed Student's t-test; Supporting Information Fig. 5).

Gamma Bursts in GFAP:TK Mice

While the aforementioned results support the idea that the absence of young adult-generated granule cells leads to increases in the amplitude of population bursting activity in the dentate gyrus, the possibility remains that this effect is due to some nonspecific effect of the focal hippocampal X-irradiation procedure, such as damage to networks of interneurons that might serve to normally inhibit this type of activity. To examine this possibility, we performed an additional set of experiments recording network activity from mice in which adult neurogenesis has been eliminated with the GFAP:TK pharmacogenetic ablation technique (Saxe et al., 2006). Mice carrying the GFAP:TK transgene and their wild-type littermates were implanted with subcutaneous ganciclovir minipumps to eliminate neural precursors expressing the transgene. The GFAP:TK transgenic mice showed significant increases in the amplitude of spontaneous gamma bursts under urethane anesthesia when compared with wild-type littermates (Fig. 3B; $P = 0.017$, two-tailed Student's t-test). The increase in amplitude was similar in magnitude to that produced with X-irradiation.

Gamma Bursts Following Perforant-Path Inactivation

Finding a reduction in the efficacy of perforant path inputs in combination with an increase in gamma burst magnitude may perhaps be surprising, given that dentate gamma bursts are thought to arise from perforant path input from the entorhinal cortex (Bragin et al., 1995; Csicsvari et al., 2003; Isomura et al., 2006). To confirm that the gamma bursts seen here were indeed dependent upon entorhinal inputs, we next examined the effects of silencing perforant path inputs on dentate network activity in the two groups. Infusion of 0.5 μl of 5 ng/μL TTX into the angular bundle abolished all dentate synaptic responses to perforant path stimulation from a twisted-wire stimulating electrode affixed 0.2-mm past the tip of the infusion cannula (Fig. 4a). Blocking ipsilateral perforant-path input dramatically reduced mean hilar gamma power in both X-rayed and sham animals (Fig. 4b, left; $P = 0.004$ for
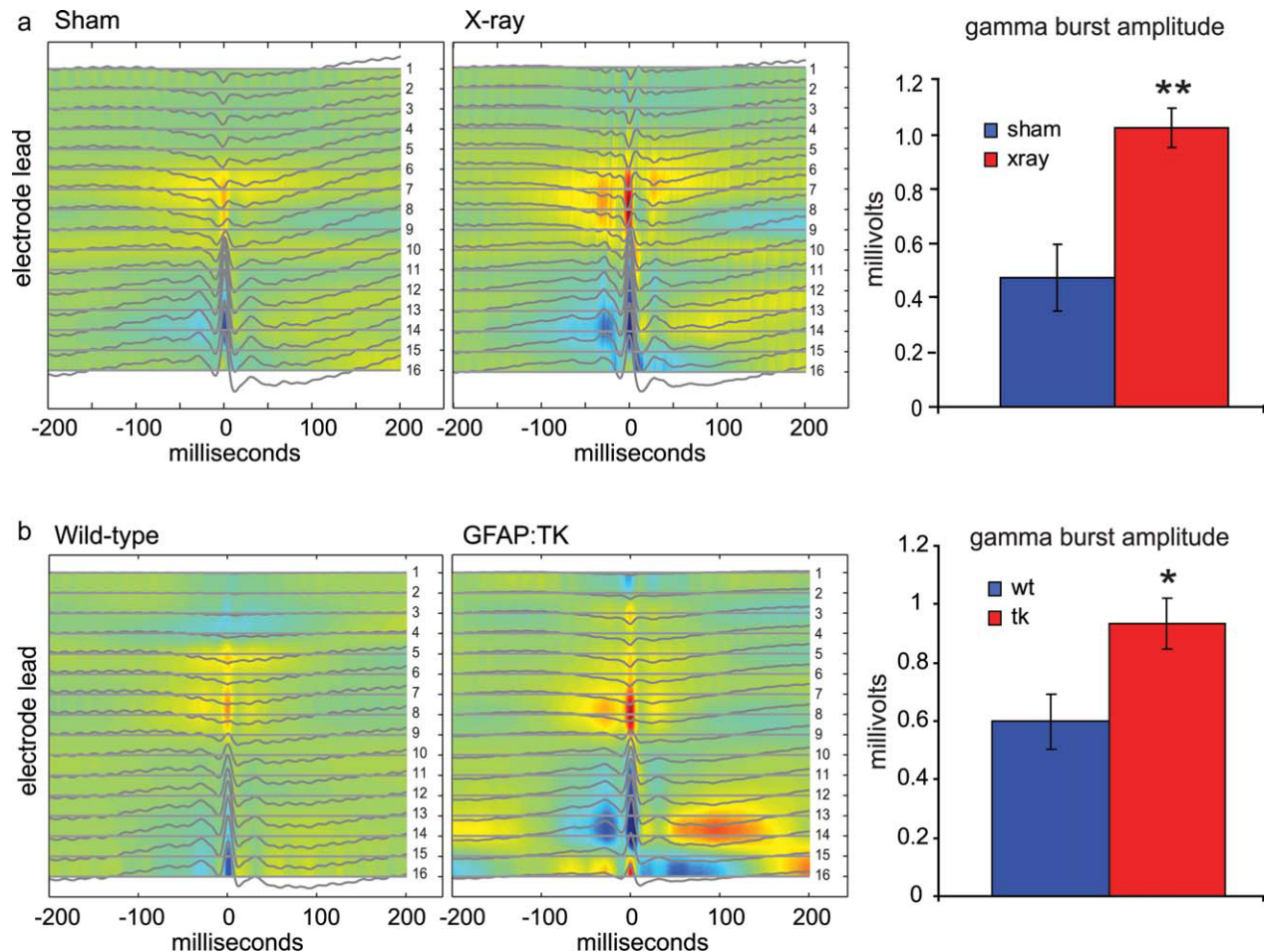
FIGURE 3. **Gamma bursts in X-irradiated and GFAP:TK animals are similar in spatial distribution to controls but increased in amplitude. (a) Average gamma burst-triggered CSDs of X-irradiated and sham animals show similar patterns of current sources and sinks. This implies that events in both groups arise due to, or are coordinated by, similar inputs. The mean amplitude of gamma bursts is significantly larger in X-irradiated animals ($n = 9$ X-ray, nine sham animals; $P = 0.001$, two-tailed Student's *t*-test). (b)** Similar to above, transgenic GFAP:TK animals given the drug ganciclovir (25 mg ml^{-1}) via subcutaneous minipump show comparable gamma burst-triggered CSDs and increased gamma burst amplitude, compared with wild-type littermates also administered ganciclovir ($n = 10$ TK, 9 wt animals; $P = 0.017$, two-tailed Student's *t*-test). [Color figure can be viewed in the online issue, which is available at wileyonlinelibrary.com.]

effect of TTX in sham, $P = 0.04$ in X-ray, two-tailed paired Student's *t*-test), and decreased the amplitude of gamma burst events (Fig. 4b, right; $P = 0.02$ for sham effect of TTX, $P = 0.03$ for X-ray, two-tailed paired Student's *t*-test). This finding confirms that the gamma bursts observed here are promoted by perforant path input, which in X-irradiated animals exhibits a reduction in mean basal synaptic transmission.

Coordination of Single-Unit Activity With Gamma Bursts

To further understand the dynamics of network activity in the sham and irradiated dentate, we next analyzed patterns of activity of individual dentate gyrus neurons during the bursting events. We clustered 25 and 34 well-separated units from seven sham and eight X-irradiated mice, respectively, and assessed the temporal relationship between unit firing and gamma burst events. Mean firing rates between the groups were similar (3.95 ± 1.63 Hz; 1.47 ± 0.47 Hz, sham/X-ray; $P = 0.085$, two-tailed Student's *t*-test), as were the percentage of spikes within bursts (Fig. 6a). Units were more likely to fire during gamma bursts in both groups (Figs. 5 and 6a). However, the timing of spikes within gamma bursts was more consistent in the X-irradiated animals; cross-correlation analysis revealed a greater tendency to fire within a short period of time relative to gamma power peaks within each event (central peak in Fig. 6b, bottom). Consistent with the modulation of gamma power by the low-frequency (θ-range) envelope within each burst, these gamma peak-triggered correlograms from X-irradiated mice revealed, in addition to this central peak, side-peaks at around 200- to 250-ms latency (Fig. 6b). Furthermore, single units from X-irradiated mice showed greater modulation of their fir-
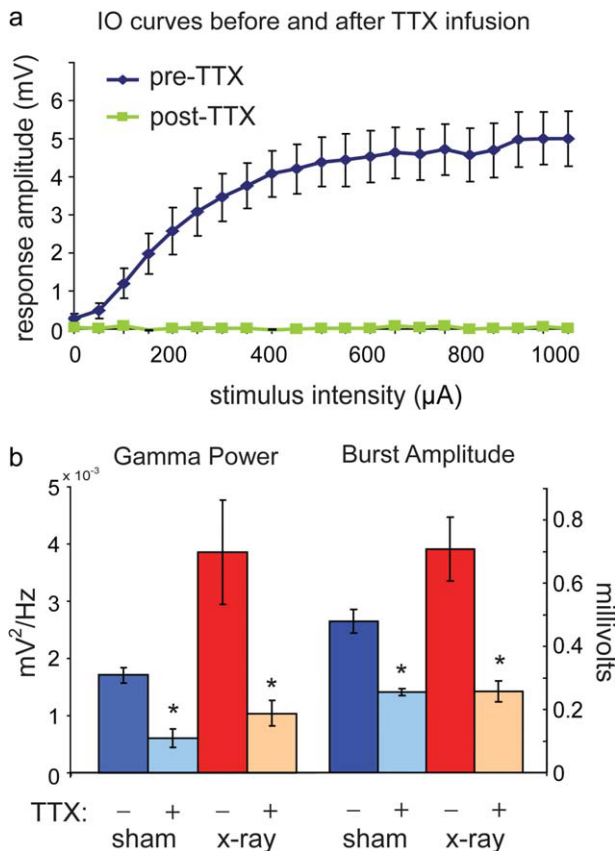
FIGURE 4.   Acute elimination of perforant-path input to the DG with TTX reduces spontaneous gamma bursts. (a) Input–output curves in response to perforant-path stimulation. Hilar evoked responses to perforant-path stimulation were completely abolished in all animals by infusion of TTX into the angular bundle. (b) Gamma power was dramatically decreased by TTX infusion in both X-irradiated and sham-treated groups ($n = 6$ X-ray, five sham animals; $P = 0.004$ for sham effect of TTX, $P = 0.04$ for X-ray, two-tailed paired Student's t-test). Gamma burst amplitude was also significantly reduced in irradiated animals ($n = 6$ X-ray, five sham animals; $P = 0.02$ for sham effect of TTX, $P = 0.03$ for X-ray, two-tailed paired Student's t-test). [Color figure can be viewed in the online issue, which is available at wileyonlinelibrary. com.]

ing by the θ-frequency components of the burst (Fig. 6c, $P = 0.01$, two-tailed Student's t-test on log-transformed data) than units from sham animals. Taken together, these results support the conclusion that animals deprived of young adult-generated neurons show an increase in synchronized activity within the dentate gyrus network, despite their weaker population synaptic responses to perforant path input.

DISCUSSION

To assess the contributions of adult-generated granule cells to dentate gyrus network physiology in vivo, we have studied both evoked and spontaneous activity from the dentate gyrus of anesthetized mice in which the generation of new neurons

in the dentate has been eliminated by hippocampal X-irradiation. These mice exhibit reduced efficacy of their perforant path inputs; an increase in the magnitude of spontaneous gamma bursts; and stronger modulation of dentate neuron firing by these bursts. Yet we also confirm that these bursts depend upon perforant path inputs, consistent with prior reports (Bragin et al., 1995; Csicsvari et al., 2003; Isomura et al., 2006). Our replication of the principal findings after pharmacogenetic ablation in GFAP:TK mice confirms that these effects are indeed due to elimination of neurogenesis rather than to nonspecific side effects of irradiation.

How do we reconcile the apparent conflict between the effects of removing adult-born neurons on evoked responses, suggesting reduced input, and on spontaneous bursts, suggesting increased response to that input? Here we suggest that our results are consistent with the hypothesis that young adult-born neurons play a modulatory role in dentate function, affecting the stability of coordinated activity in the network as a whole.

The decreased dentate response to perforant path input is consistent with a loss of young adult-generated neurons after X-irradiation, since these neurons have been shown to be more highly excitable and subject to weaker inhibition than mature granule cells (Doetsch and Hen, 2005; Esposito et al., 2005; Ge et al., 2008; Mongiat et al., 2009). The evoked field response to perforant path input is primarily a function of direct feedforward input to the entire population of young and mature neurons. The loss of the disproportionately strong responses of young neurons through X-irradiation would therefore be expected to reduce the evoked response, resulting in the altered input/output curve seen here. It is interesting that previous experiments in the slice preparation have not shown such a decrease in field responses after irradiation (Saxe et al., 2006), suggesting that this effect may only be observable under stimulation conditions present in vivo.

Paradoxically, we find that the lack of these more excitable young neurons increases spontaneous network activity. This finding suggests that these neurons modulate networks of mature cells in the dentate gyrus, and do so in a manner that is not a simple function of their own excitability. We propose two nonmutually exclusive hypotheses by which young neurons might negatively modulate network activity in the dentate. First, young neurons might preferentially activate inhibitory interneurons. Thus, once excited by perforant path input, young neurons would dampen down subsequent dentate activity. Second, young neurons might decrease excitation of mature granule cells, by directly competing with them for excitatory input. The evidence for and against these hypotheses is discussed below.

There is some evidence to support the possibility that newly born neurons might selectively stimulate networks of interneurons in the hilus and CA3 (Fig. 7b, Part 1). Mossy fiber axons from granule cells target a number of different cell types, both at intermediate distances in the hilus as well as at their terminus in CA3. In fact, as far as numbers are concerned, hilar interneurons are the major target of connections from granule cells (Acsady et al., 1998). While axons of young adult-gener-
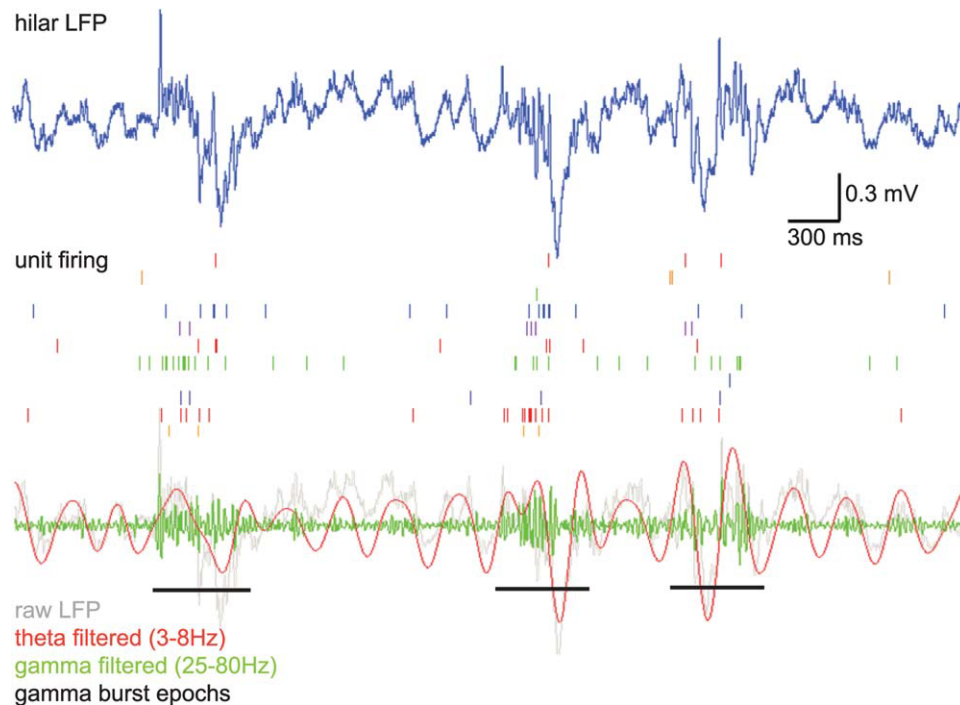
FIGURE 5. Dentate neurons tend to fire with gamma bursts. Raster plots of unit firing during gamma burst epochs show increases in firing rate during bursting events. Top panel: Raw LFP from probe contact located in the hilus. Middle panel: Raster plots from a selection of units recorded simultaneously with the above LFP. Bottom panel: LFP trace filtered for theta (3–8 Hz) (red) and gamma (25–80 Hz) (green). The raw trace is repeated in gray for comparison. Gamma burst epochs as identified by a gamma power algorithm (see Methods and Supporting Information Fig. 4) are indicated in black. [Color figure can be viewed in the online issue, which is available at wileyonlinelibrary.com.]

ated granule cells do form functional mossy fiber boutons onto CA3 pyramidal cells from an early developmental stage, these specialized synapses are not fully mature until after the adult-born neurons are around 8-weeks old (Faulkner et al., 2008; Toni et al., 2008), when these neurons should no longer be hyperexcitable (Ge et al., 2007; Mongiat et al., 2009). It is not known whether the numerous filopodial connections of mossy fiber axons onto most interneurons follow a similar delayed development in adult-generated granule cells. Such inputs however are typically more robust than those onto CA3 pyramidal cells (Scharfman et al., 1990; Mori et al., 2004, 2007) and therefore may be relevant at earlier stages than the specialized mossy fiber synapses, while young neurons are still highly excitable. These characteristics of the dentate circuit allow for the possibility that interneurons may be more effectively driven by young adult-born neurons. Thus, these young neurons may have a net inhibitory effect on the more complex spontaneous network activity despite being themselves more excited by artificially evoked, single-pulse perforant path input.

Alternately, young neurons may decrease excitation of mature neurons in the granule cell layer. Competition with mature neurons for the perforant path connections that drive gamma bursts (Fig. 7b, Part 2) could explain why elimination of young neurons increases gamma bursts, which invoke a feedback excitatory-inhibitory circuit in the dentate gyrus and hilus. After eliminating neurogenesis, the lack of competition from the nascent synapses of immature granule cells may result in more

effective perforant path stimulation of mature granule cells, whose activation is then required for coordinated network activity. Consistent with this hypothesis, it has been proposed that young neurons invade, and may replace, afferent connections onto mature neurons (Toni et al., 2007). These connections onto mature granule cells likely play some role in the amplitude of gamma bursts, and may be disrupted by competing synapses from young neurons. The hypothesis that new neurons decrease gamma bursts by disrupting patterns of perforant path connections onto mature granule cells is also consistent with the recent finding that X-irradiation leads to prolonged LTP in the dentate gyrus in behaving rats (Kitamura et al., 2009). Notably, LTP induction in vivo leads to increases in gamma burst-like activity (Bikbaev and Manahan-Vaughan, 2007). Increased gamma network activity in X-irradiated animals may therefore be due to sustained potentiation of perforant-path synapses onto mature granule cells, enabled by the absence of young neurons which would otherwise disrupt the strong connections that generate this activity.

Regardless of the specific mechanism, the current results provide evidence that the integration of young neurons into neural circuits in the adult dentate gyrus has feedback effects on network physiology in the region in vivo that cannot be simply explained by prior in vitro experiments on the physiology of single neurons. It is perhaps surprising that eliminating such a relatively small subpopulation might have effects upon the body of granule cells as a whole. The stability of network states
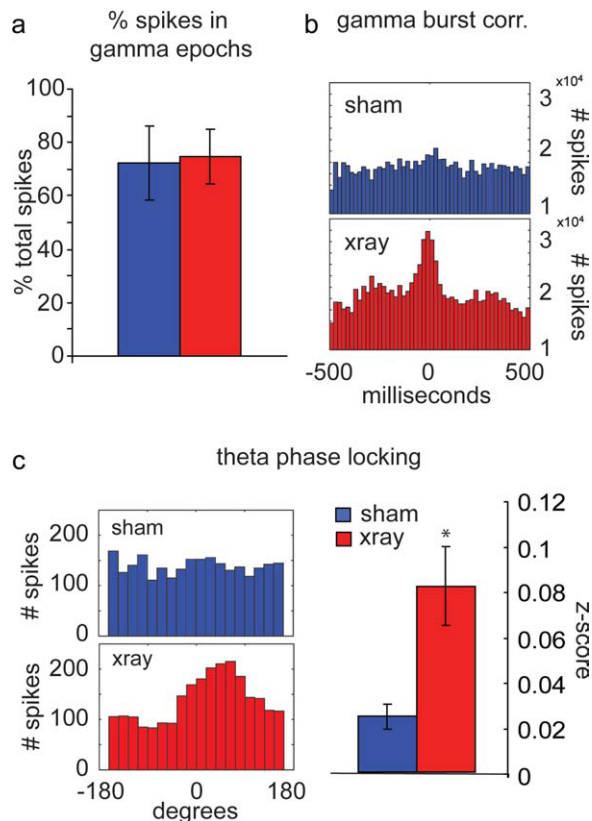
FIGURE 6.   X-irradiation increases spike-LFP synchrony within gamma bursts. (a) Percentage of spikes occurring during gamma bursts in sham (blue) and x-irradiated (red) animals. In both groups, most spikes occurred during gamma bursts. Mean ± S.E.M. (b) γ-burst-triggered peri-event histograms of all spikes recorded from all animals in sham (blue) and X-irradiated (red) groups. Spikes in X-rayed animals occur preferentially at the peaks of gamma power during gamma bursts while sham animals show no such preference. Note the side peaks at 250- to 350-ms latency indicating prominent θ-frequency modulation in the X-irradiated animals. (c) Left panel, θ-phase distribution histograms for spikes recorded from sham and x-irradiated animals; 100 spikes from each single unit were used ($n = 34$ units in X-irradiated animals, 25 units in sham animals). Theta phase was calculated from the LFP recorded in the hilus. Right panel, mean Rayleigh's z-statistic (a measure of the strength of phase locking) from neurons recorded from sham and X-irradiated animals ($P = 0.01$, two-tailed Student's t-test on log transformed data). [Color figure can be viewed in the online issue, which is available at wileyonlinelibrary.com.]

in the dentate may however be exquisitely sensitive to such incremental changes in the properties or types of neurons constituting the circuit, as has been suggested in neural network models of seizure activity in the hippocampus (Bogaard et al., 2009). The current work therefore provides an additional level of complexity in thinking about how the population of young neurons affects processing in the dentate gyrus. While we still do not know how these changes in synchronous activity of granule cells in the dentate under urethane anesthesia relate to neural activity during behavior, the disruption of patterns of coordinated activity in mature granule cells helps explain how abolition of neurogenesis could consequently affect computa-

tional roles of the dentate gyrus, such as pattern separation (McHugh et al., 2007; Treves et al., 2008; Clelland et al., 2009).

As a whole, these findings provide preliminary support for the hypothesis that young adult-generated granule cells may serve to modulate processing in the population of mature granule cells—a circuit-wide mechanism for modifying the overall tone of activity in the dentate gyrus in response to changing environmental conditions. For example, stress, which decreases adult hippocampal neurogenesis, and environmental enrichment, which increases it, would be predicted to influence dentate activity in opposite directions. Disruption of the modulatory function of adult neurogenesis by factors such as stress
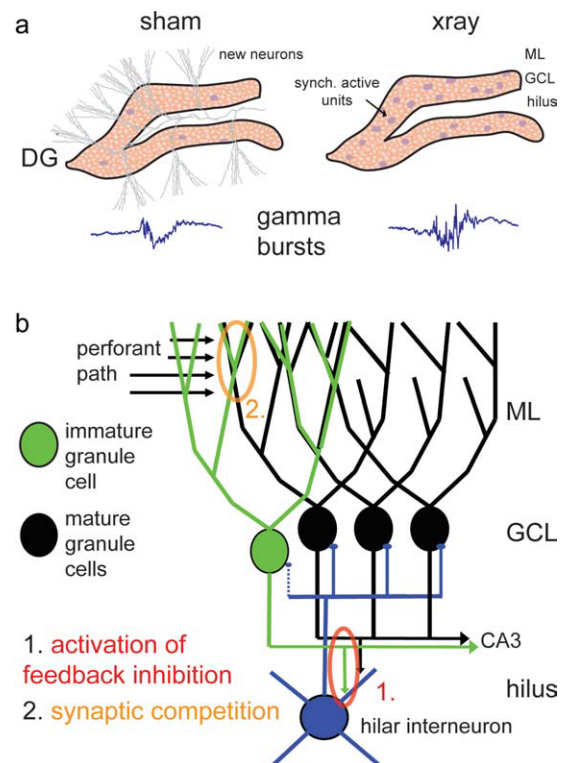
FIGURE 7.   Young neurons destabilize network activity in the intact dentate gyrus. (a.) Schematic of the dentate gyrus, depicting effect of immature granule cells on correlated cell firing and gamma bursting activity. Left panel: in the presence of young adult-born granule cells (gray), the dentate gyrus shows only modest correlations of cell firing (purple somata) and smaller gamma bursts (example LFP at lower left). Right panel: after eliminating adult neurogenesis with X-irradiation, young neurons are no longer present and we observe increased correlations in cell firing and amplitude of gamma bursts. (b) Model of the effects of young neurons on dentate activity. We propose two possible explanations for the effects of immature adult-generated granule cells on neuronal phase locking to gamma bursts and gamma burst amplitude: (1) (red) immature granule cells may fire more easily, increasing the tone of feedback interneurons in the hilus that subsequently clamp down on gamma bursting activity. (2) (yellow) young neurons may compete for strong perforant path connections with mature cells, which normally drive gamma bursting events after barrages of entorhinal cortical input.[Color figure can be viewed in the online issue, which is available at wileyonlinelibrary.com.]

may consequently contribute to the decrease in cognitive flexibility that characterizes many psychiatric disorders, such as anxiety and depression.

Acknowledgments

REFERENCES

Acsady L, Kamondi A, Sik A, Freund T, Buzsaki G. 1998. GABAergic cells are the major postsynaptic targets of mossy fibers in the rat hippocampus. J Neurosci 18:3386–3403.

Aimone JB, Wiles J, Gage FH. 2006. Potential role for adult neurogenesis in the encoding of time in new memories. Nat Neurosci 9:723–727.

Aimone JB, Wiles J, Gage FH. 2009. Computational influence of adult neurogenesis on memory encoding. Neuron 61:187–202.

Altman J, Das GD. 1965. Autoradiographic and histological evidence of postnatal hippocampal neurogenesis in rats. J Comp Neurol 124:319–335.

Becker S, Wojtowicz JM. 2007. A model of hippocampal neurogenesis in memory and mood disorders. Trends Cogn Sci 11:70–76.

Bikbaev A, Manahan-Vaughan D. 2007. Hippocampal network activity is transiently altered by induction of long-term potentiation in the dentate gyrus of freely behaving rats. Front Behav Neurosci 1:7.

Bogaard A, Parent J, Zochowski M, Booth V. 2009. Interaction of cellular and network mechanisms in spatiotemporal pattern formation in neuronal networks. J Neurosci 29:1677–1687.

Bragin A, Jando G, Nadasdy Z, Hetke J, Wise K, Buzsaki G. 1995. Gamma (40–100 Hz) oscillation in the hippocampus of the behaving rat. J Neurosci 15(1, Part 1):47–60.

Clelland CD, Choi M, Romberg C, Clemenson GD Jr, Fragniere A, Tyers P, Jessberger S, Saksida LM, Barker RA, Gage FH, et al. 2009. A functional role for adult hippocampal neurogenesis in spatial pattern separation. Science 325:210–213.

Csicsvari J, Jamieson B, Wise KD, Buzsaki G. 2003. Mechanisms of gamma oscillations in the hippocampus of the behaving rat. Neuron 37:311–322.

David DJ, Samuels BA, Rainer Q, Wang JW, Marsteller D, Mendez I, Drew M, Craig DA, Guiard BP, Guilloux JP, et al. 2009. Neurogenesis-dependent and -independent effects of fluoxetine in an animal model of anxiety/depression. Neuron 62:479–493.

Deng W, Saxe MD, Gallina IS, Gage FH. 2009. Adult-born hippocampal dentate granule cells undergoing maturation modulate learning and memory in the brain. J Neurosci 29:13532–13542.

Doetsch F, Hen R. 2005. Young and excitable: The function of new neurons in the adult mammalian brain. Curr Opin Neurobiol 15:121–128.

Dudek FE, Deadwyler SA, Cotman CW, Lynch G. 1976. Intracellular responses from granule cell layer in slices of rat hippocampus: Perforant path synapse. J Neurophysiol 39:384–393.

Esposito MS, Piatti VC, Laplagne DA, Morgenstern NA, Ferrari CC, Pitossi FJ, Schinder AF. 2005. Neuronal differentiation in the adult hippocampus recapitulates embryonic development. J Neurosci 25:10074–10086.

Faulkner RL, Jang MH, Liu XB, Duan X, Sailor KA, Kim JY, Ge S, Jones EG, Ming GL, Song H, et al. 2008. Development of hippocampal mossy fiber synaptic outputs by new neurons in the adult brain. Proc Natl Acad Sci USA 105:14157–14162.

Ge S, Yang CH, Hsu KS, Ming GL, Song H. 2007. A critical period for enhanced synaptic plasticity in newly generated neurons of the adult brain. Neuron 54:559–566.

Ge S, Sailor KA, Ming GL, Song H. 2008. Synaptic integration and plasticity of new neurons in the adult hippocampus. J Physiol 586:3759–3765.

Isomura Y, Sirota A, Ozen S, Montgomery S, Mizuseki K, Henze DA, Buzsaki G. 2006. Integration and segregation of activity in entorhinal-hippocampal subregions by neocortical slow oscillations. Neuron 52:871–882.

Jones MW, Peckham HM, Errington ML, Bliss TV, Routtenberg A. 2001. Synaptic plasticity in the hippocampus of awake C57BL/6 and DBA/2 mice: Interstrain differences and parallels with behavior. Hippocampus 11:391–396.

Kee N, Teixeira CM, Wang AH, Frankland PW. 2007. Preferential incorporation of adult-generated granule cells into spatial memory networks in the dentate gyrus. Nat Neurosci 10:355–362.

Kempermann G, Kuhn HG, Gage FH. 1997. Genetic influence on neurogenesis in the dentate gyrus of adult mice. Proc Natl Acad Sci USA 94:10409–10414.

Kitamura T, Saitoh Y, Takashima N, Murayama A, Niibori Y, Ageta H, Sekiguchi M, Sugiyama H, Inokuchi K. 2009. Adult neurogenesis modulates the hippocampus-dependent period of associative fear memory. Cell 139:814–827.

Laplagne DA, Esposito MS, Piatti VC, Morgenstern NA, Zhao C, van Praag H, Gage FH, Schinder AF. 2006. Functional convergence of neurons generated in the developing and adult hippocampus. PLoS Biol 4:e409.

Malberg JE, Eisch AJ, Nestler EJ, Duman RS. 2000. Chronic antidepressant treatment increases neurogenesis in adult rat hippocampus. J Neurosci 20:9104–9110.

McHugh TJ, Jones MW, Quinn JJ, Balthasar N, Coppari R, Elmquist JK, Lowell BB, Fanselow MS, Wilson MA, Tonegawa S. 2007. Dentate gyrus NMDA receptors mediate rapid pattern separation in the hippocampal network. Science 317:94–99.

Meshi D, Drew MR, Saxe M, Ansorge MS, David D, Santarelli L, Malapani C, Moore H, Hen R. 2006. Hippocampal neurogenesis is not required for behavioral effects of environmental enrichment. Nat Neurosci 9:729–731.

Mongiat LA, Esposito MS, Lombardi G, Schinder AF. 2009. Reliable activation of immature neurons in the adult hippocampus. PLoS ONE 4:e5320.

Mori M, Abegg MH, Gahwiler BH, Gerber U. 2004. A frequency-dependent switch from inhibition to excitation in a hippocampal unitary circuit. Nature 431:453–456.

Mori M, Gahwiler BH, Gerber U. 2007. Recruitment of an inhibitory hippocampal network after bursting in a single granule cell. Proc Natl Acad Sci USA 104:7640–7645.

Nakashiba T, Young JZ, McHugh TJ, Buhl DL, Tonegawa S. 2008. Transgenic inhibition of synaptic transmission reveals role of CA3 output in hippocampal learning. Science 319:1260–1264.

Namgung U, Valcourt E, Routtenberg A. 1995. Long-term potentiation in vivo in the intact mouse hippocampus. Brain Res 689:85–92.

Nicholson C, Freeman JA. 1975. Theory of current source-density analysis and determination of conductivity tensor for anuran cerebellum. J Neurophysiol 38:356–368.

Sahay A, Hen R. 2007. Adult hippocampal neurogenesis in depression. Nat Neurosci 10:1110–1115.

Santarelli L, Saxe M, Gross C, Surget A, Battaglia F, Dulawa S, Weisstaub N, Lee J, Duman R, Arancio O, et al. 2003. Requirement of hippocampal neurogenesis for the behavioral effects of antidepressants. Science 301:805–809.

Saxe MD, Battaglia F, Wang JW, Malleret G, David DJ, Monckton JE, Garcia AD, Sofroniew MV, Kandel ER, Santarelli L, et al.

2006. Ablation of hippocampal neurogenesis impairs contextual fear conditioning and synaptic plasticity in the dentate gyrus. Proc Natl Acad Sci USA 103:17501–17506.

Scharfman HE, Kunkel DD, Schwartzkroin PA. 1990. Synaptic connections of dentate granule cells and hilar neurons: Results of paired intracellular recordings and intracellular horseradish peroxidase injections. Neuroscience 37:693–707.

Schmidt-Hieber C, Jonas P, Bischofberger J. 2004. Enhanced synaptic plasticity in newly generated granule cells of the adult hippocampus. Nature 429:184–187.

Snyder JS, Kee N, Wojtowicz JM. 2001. Effects of adult neurogenesis on synaptic plasticity in the rat dentate gyrus. J Neurophysiol 85:2423–2431.

Snyder JS, Hong NS, McDonald RJ, Wojtowicz JM. 2005. A role for adult neurogenesis in spatial long-term memory. Neuroscience 130:843–852.

Tashiro A, Makino H, Gage FH. 2007. Experience-specific functional modification of the dentate gyrus through adult neurogenesis: A critical period during an immature stage. J Neurosci 27:3252–3259.

Toni N, Teng EM, Bushong EA, Aimone JB, Zhao C, Consiglio A, van Praag H, Martone ME, Ellisman MH, Gage FH. 2007. Synapse formation on neurons born in the adult hippocampus. Nat Neurosci 10:727–734.

Toni N, Laplagne DA, Zhao C, Lombardi G, Ribak CE, Gage FH, Schinder AF. 2008. Neurons born in the adult dentate gyrus form functional synapses with target cells. Nat Neurosci 11:901–907.

Treves A, Tashiro A, Witter ME, Moser EI. 2008. What is the mammalian dentate gyrus good for? Neuroscience 154:1155–1172.

Wang S, Scott BW, Wojtowicz JM. 2000. Heterogenous properties of dentate granule neurons in the adult rat. J Neurobiol 42:248–257.

Wigstrom H, Gustafsson B. 1983. Large long-lasting potentiation in the dentate gyrus in vitro during blockade of inhibition. Brain Res 275:153–158.

Zhang CL, Zou Y, He W, Gage FH, Evans RM. 2008. A role for adult TLX-positive neural stem cells in learning and behaviour. Nature 451:1004–1007.